Journal of Thermal Analysis and Calorimetry, Vol. 88 (2007) 2, 431–435

ETS-10 SYNTHESIZED FROM GELS WITH DODECYLTRIMETHYLAMMONIUM BROMIDE
Thermal and morphological analysis

N. A. Turta[1], *D. Vuono*[2], *P. De Luca*[2*], *N. Bilba*[1] *and A. Nastro*[2]

[1]Al. I. Cuza, University of Iasi, Faculty of Chemistry, Department of Physical Chemistry, Theoretical and Materials Chemistry
11 Carol I Bd. 700506 Iasi, Romania
[2]Department of Pianificazione Territoriale, University of Calabria, via P. Bucci, 87036 Arcavacata di Rende (CS), Italy

The aim of this paper is to define the characteristics of crystalline phase ETS-10 obtained from gel with dodecyltrimethylammonium bromide, as an organic template. ETS-10 zeolites has been synthesised under hydrothermal conditions from gels of composition $5Na_2O$–3KF–TiO_2–6.4HCl– xC_{12}TMAB –$7.45SiO_2$–$197.5H_2O$ (where x=0.0, 0.25, 0.55, 1.0 and 1.5) with dodecyltrimethylammonium bromide. The crystalline phases synthesised with organic salt have an exothermal peak at ca. 360°C, due to the degradation of organic entrapped in the porous structure. Physical-chemical properties of C_{12}TMAB -ETS-10 are studied by XRD, SEM and thermal analyses.

Keywords: *dodecyltrimethylammonium, ETS-10, kinetic curves, molecular sieves, organic template, zeolites*

Introduction

Zeolites constitute a major class of natural and synthetic aluminosilicate, crystalline, microporous materials. They exhibit a rigid three-dimensional atomic structure, consisting of a network of interconnected tunnels and cages which are built from SiO_4 and AlO_4 tetrahedra [1–4]. Their uniform molecular size pores give to zeolites the capacity to separate mixtures of substances on the molecular level, which allows them to be termed molecular sieves. Because of these properties, the zeolites have found a wide spectrum of environmental and industrial applications as sorbents, ion exchangers, shape-selective catalysts or catalyst supports [5–9].

The first information related to microporous titanosilicate goes back to 1967 when Young described the synthesis of a titanosilicate under conditions similar to those used for the aluminosilicate zeolites [10].

Among the microporous crystalline titanosilicates containing octahedral Ti and tetrahedral Si, the ETS-4 and ETS-10 structures, first synthesized by Kuznicki in 1989, are the most important ones [11, 12]. These materials show a good catalytic activity and can also be used as molecular sieves or ion exchanger. Furthermore, ETS-10 exhibits good thermal stability up to ca. 650°C in air. The structure of ETS-10 has been determined by Anderson *et al.* [13, 14].

The ETS-10 structure is composed of lateral SiO_4 tetrahedra and TiO_6 octahedra joined by oxygen bridges and the pore structure consists of 12, 7, 5 and 3 rings and has a dimensional wide pore channel system, whose minimum diameter defined by 12-membered rings are ellipsoidal with 8.6·9.2 Å dimensions [14]. The highly disordered structure can be considered as an intergrowth of two-end member polymorphs (the chiral tetragonal polymorph A and the monoclinic polymorph B). The most interesting aspects of the structure of ETS-10 are that it contains several –O–Ti–O–Ti–O– chains surrounded by a silicate ring structure. ETS-10 has a tetragonal symmetry with a unit cell chemical composition $M_2TiSi_5O_{13}\cdot nH_2O$ (M=Na^+, K^+).

ETS-10 has been synthesized under hydrothermal conditions (temperatures from ca. 180 to 250°C, synthesis time from 16 h to 30 days, pH of initial gel in the range 10–12), without any organic template, using $TiCl_3$ [11, 13, 14, 18–20], $TiCl_4$ [15–17], TiF_4 [20, 21], TiO_2-anatas [18, 20], TiO_2 nano-sized [20, 22], $Ti_2(SO_4)_3$ [23], $(NH_4)_2TiF_6$ [20] as Ti sources and sodium silicate solution, fumed or colloidal silica as Si sources, in presence of NaOH, NaCl, KCl and KF. The crystallization field of ETS-10 depends on the quantities of Na_2O, K_2O, TiO_2 and SiO_2 in initial gel, the type of Ti precursors, and on synthesis conditions, such as pH, etc. ETS-10 is easily contaminated with other phase [24].

ETS-10 has also been synthesized with organic molecules such as tetramethylammonium chloride [25–27], pyrrolidine, tetraethylammonium chloride, tetrapropylammonium bromide, 1,2-diaminoethane [28],

---

[*] Author for correspondence: p.deluca@unical.it

1388–6150/$20.00

Akadémiai Kiadó, Budapest, Hungary
Springer, Dordrecht, The Netherlands

choline chloride and bromide salt of hexaethyldiquat-5 [29] and salts of tetraalkylammonium and ethanolamine [30, 31]. Pavel *et al.* examined the crystallisation kinetics starting from gels containing tetraalkylammonium bromides [31, 32]. Vuono *et al.* study the physico-chemical properties of ET(Zr)S-10 obtained from a gel containing different amounts of Zr [33]. Onyestiak *et al.* synthesized Cd- and Zn-ferrierites can be obtained by reacting the corresponding metal and H-ferrierite in the solid phase [34]. In this paper the crystallization kinetics have been examined starting from gels containing cethyltrimethylammonium bromides. The final crystalline samples were characterized by XRD, TG/DTG/DSC and SEM.

Experimental

Synthesis of titanium silicate ETS-10 and C_{12}TMAB-ETS-10 was carried out from starting gels with molar composition: $5Na_2O–3KF–TiO_2–6.4HCl–xC_{12}TMAB–7.45SiO_2–197.5H_2O$ (where x= 0.0, 0.25, 0.55, 1.0 and 1.5) with C_{12}TAB=dodecyltrimethylammonium bromide, (Aldrich). The reaction mixtures were prepared by mixing an acidic aqueous solution obtained by dissolving KF (40 mass%, Merck), $TiCl_4$ (50 mass%, Merck), HCl (37 mass%, Merck) and distilled water with a basic aqueous solution obtained from sodium silicate (8 mass% Na_2O, 27 mass% SiO_2, Merck), NaOH (50 mass%, BDH), C_{12}TMAB (Aldrich) and distilled water. The experiments were carried out in PTFE.lined Morey type stainless steel autoclave without stirring at temperature of 190±2°C.

The powder diffraction patterns were recorded on a Philips PW 1830 diffractometer using CuK_α radiation. The scanning speed was 0.02° s^{-1} in the range of 5–45° 2θ. The thermal analysis was carried out on a Netzsch 429 instrument. The temperature range was 20–750°C with a heating rate of 10°C min^{-1} in static air. The morphology of the crystals was studied on a SEM Stereoscan 360 S scanning electron microscope. The aim of this study is to determine the physical-chemical properties of C_{12}TMAB-ETS-10.

Results and discussion

Figure 1 shows the field of crystallisation of ETS phases as a function of C_{12}TMAB amount in initial gels. It can be noted that pure ETS-10 is synthesised at 0.8–1 moles of natrium oxide, while the ETS-4 is synthesised with higher amount of natrium. The C_{12}TMAB amount does not affect the crystallisation of both molecular sieves. In fact, the crystalline phases are present in the range 0.25–1.5 moles of C_{12}TMAB. Amorphous is produced at ca. 0.5–0.7 moles of Na_2O. The pH value of initial gel is less than 10.8.

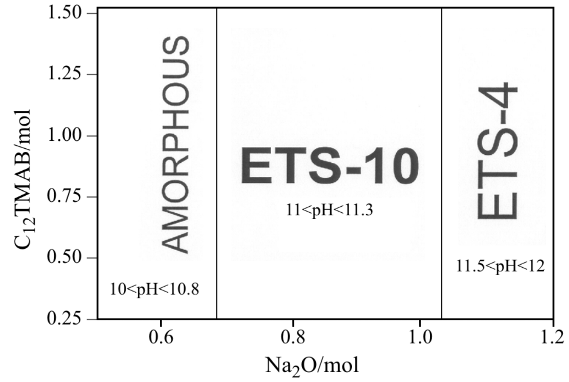

Fig. 1 Crystallization fields of the phases obtained from system: $yNa_2O–3KF–TiO_2–6.4HCl–xC_{12}TMAB–7.45SiO_2–197.5H_2O$ with x=0.25, 0.55, 1.0, 1.5 and y=0.4, 0.8, 1.0, 1.2; Reaction time: 3 days; temperature: 190°C

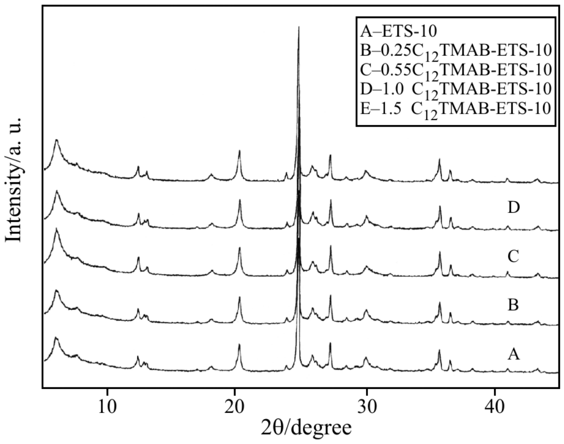

Fig. 2 XRD patterns of products obtained from: $5Na_2O–3KF–TiO_2–6.4HCl–xC_{12}TMAB–7.45SiO_2––197.5H_2O$

The XRD patterns of the titanosilicates ETS-10 synthesized with and without C_{12}TMAB template are shown in Fig. 2. The XRD patterns are in good agreement with the published ETS-10 data [10, 20] indicating the presence of a single phase.

In order to investigate the effect of C_{12}TMAB template on the crystallization of ETS-10, four samples of ETS-10 were synthesized with different content (x) of C_{12}TMAB.

The evolution of the cristallinity, calculated from XRD data are depicted in Fig. 3. The kinetic curves of C_{12}TMAB-ETS-10 exhibit a typical sigmoid shape of process involving two stages, one is induction stage characterized by induction time (t_i) and the other is crystal growth characterized by rate of crystallization (R). Induction time (t_i) is an arbitrary point that corresponds to the time, in h, for the appearance of 4% crystallinity.

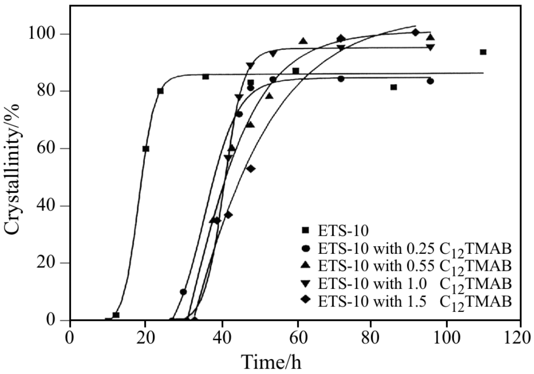

Fig. 3 Crystallization curves of the phases obtained from gels of the compositions $5Na_2O–3KF–TiO_2–6.4HCl–xC_{12}TMAB––7.45SiO_2–197.5H_2O$ at 190°C

Rate of crystallization (R) expressed in % h^{-1} is computed from the crystallization curves as the steepest slope as a function of time. The results suggest that presence of C_{12}TMAB in the gels prolong the induction period by comparison with the ETS-10 synthesized without organic template. The ETS-10 crystallization starts at ca. 10 h, while the C_{12}TMAB-ETS-10 curves start between 27 and 33 h. The organic adding in reaction mixtures seems to have an effect on kinetic curves. The crystallinity of samples synthesized with $x>0.25$ moles attained 100% after 90 h at 190°C.

Table 1 presents the kinetic parameters for crystallization curves studied above. The induction times increase from 12.5 h for ETS-10 without organic to 33.6 h for C_{12}TMAB-ETS-10 with 1.0 and 1.5 moles of organic. The induction times for samples with C_{12}TMAB increase slowly with increase of moles of C_{12}TMAB. The crystallization rates (slope of linear part of sigmoidal curve) tend to decrease as a function of increasing organic salt in initial gel.

Figure 4 shows the DTG curves of different C_{12}TMAB-ETS-10 samples. DTG curves are compared with that of ETS-10 obtained without organic. It can be noted that a new peak appears at ca. 360°C for samples produced with organic salt in initial gel. This peak means that C_{12}TMAB molecules are incorporated into channel system of ETS-10. The ETS-10 has the only peak at ca. 110°C due to the zeolitic water loss.

Table 1 Kinetic parameters and crystal characterization for systems of composition: $5Na_2O–3KF–TiO_2–6.4HCl––xC_{12}TMAB –7.45SiO_2–197.5H_2O$ at 190°C

C_{12}TMAB/mol	t_i/h	R/% h^{-1}
0.00	12.5	9.70
0.25	28.4	4.10
0.55	31.5	5.00
1.00	33.6	7.00
1.50	33.6	2.70

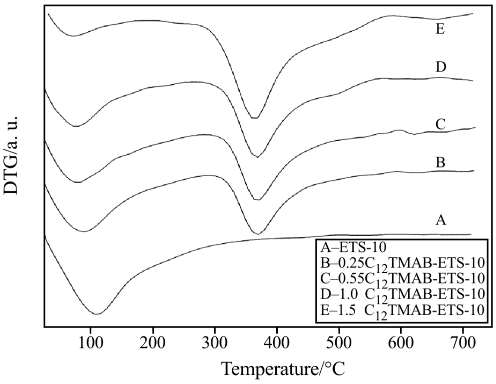

Fig. 4 DTG curves of ETS-10 and of products obtained from: $5Na_2O–3KF–TiO_2–6.4HCl–xC_{12}TMAB–7.45SiO_2––197.5H_2O$ at 190°C. Reaction time: 3 days

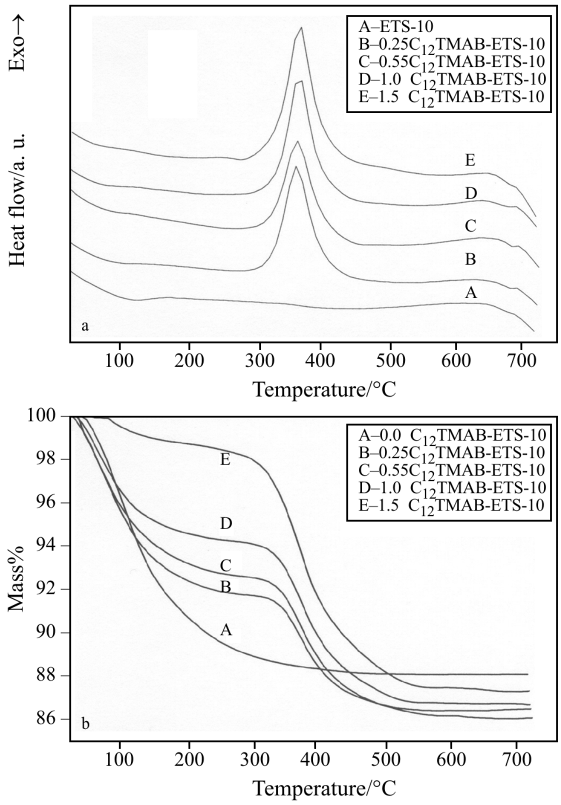

Fig. 5 a– DSC and b– TG curves of products obtained from: $5Na_2O–3KF–TiO_2–6.4HCl–xC_{12}TMAB–7.45SiO_2––197.5H_2O$ at 190°C. Reaction time: 3 days; temperature:190°C

In Fig. 5 are shown the DSC and TG curves of the studied samples (ETS-10 with and without template). The crystalline phases synthesised with organic salt have an exothermal peak at ca. 360°C, due to the degradation of organic probably bonded to the structure.

The zeolitic and organic mass loss as a function of organic amounts in initial gels are presented in Table 2. The water in pores decreases with template in initial gel, while the organic increases. It is very

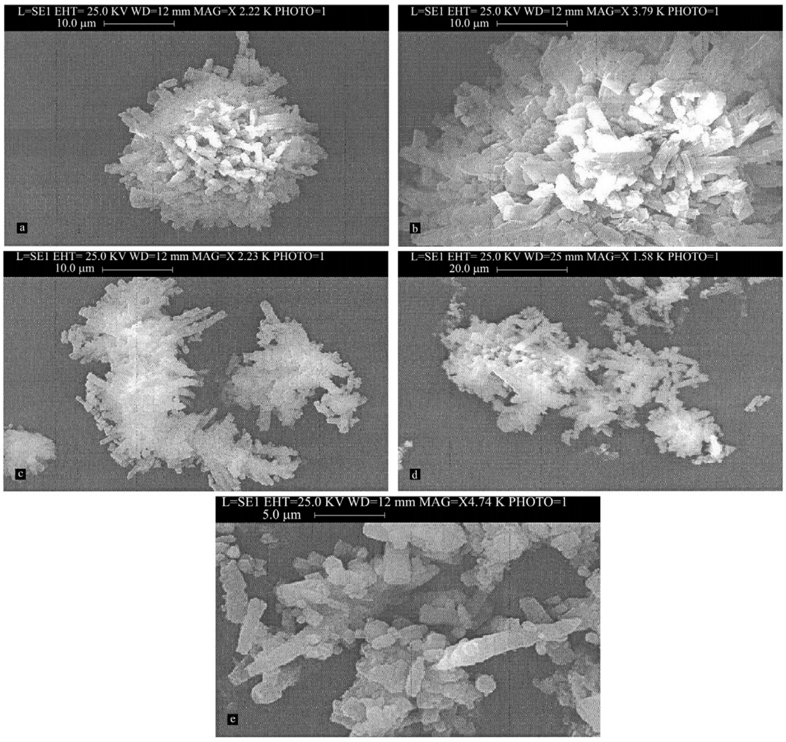

Fig. 6 SEM pictures of solid products obtained from the gel with the composition: $5Na_2O–3KF–TiO_2–6.4HCl–xC_{12}TMAB–7.45SiO_2–197.5H_2O$; a– x=0.25, b– x=0.55, c– x=1.0, d– x=1.5 and e– x=0.0; reaction time: 3 days; temperature: 190°C

Table 2 Thermal analysis data of the C_{12}TMAB-ETS-10 samples synthesized at 190°C for 72 h

C_{12}TMAB/ mol	Water content/%	Organic content/%	Total loss/%
0	11.88	–	11.88
0.25	8.25	5.24	13.49
0.55	7.38	6.51	13.89
1.0	5.73	7.46	13.19
1.5	1.38	11.32	12.7

Table 3 DSC peaks of C_{12}TMAB-ETS-10 samples synthesized at 190°C for 72 h

C_{12}TMAB/mol	Peak I/°C	Peak II/°C
0	125.1	–
0.25	90.4	361.8
0.55	85.9	362.6
1.0	78.2	365.5
1.5	70.6	365.9

interesting to note that the organic salt bonded to the structure substitutes the zeolitic water. The organic content at 1.5 moles of C_{12}TMAB in initial gel is nearly equal to the water content of ETS-10. This behaviour is due to the steric hindrance produced by the organic salt filling the pores, while the water cannot enter.

The micrographs of samples made with different quantities of C_{12}TMAB samples are shown in Fig. 6. The morphology of the obtained phases is not clear and agglomerates are formed. The crystals dimensions do not vary as a function of C_{12}TMAB contents. The length of C_{12}TMAB-ETS-10 crystals is between 4 and 3 µm.

Conclusions

It is possible to synthesize molecular sieve ETS-10 adding C_{12}TMAB salt as template in initial gels.

Thermal analysis clearly shows the thermal decomposition of organic additives incorporated into the channels of ETS-10. The DSC curves of ETS-10 obtained with C_{12}TMAB highlight the presence of an exothermal peak at 360°C due to the organic degradation in the pores.

The TG data show that the water content obviously decreases increasing organic amount in the initial gel since it is occupying a consistent part of the channels. Kinetics studies show that the induction times increasing significantly with organic template. Crystal morphology remains substantially unvaried.

References

1 C. C. Pavel, K. Popa, N. Balba, A. Cecal, D. Cozma and A. Pui, J. Radioanal. Nucl. Chem., 258 (2003) 243.
2 D. W. Breck, Zeolite Molecular Sieves: Structure, Chemistry and Use, John Wiley, New York 1974.
3 S. L. Burkett and M. E. Davis, Chem. Mater., 7 (1995) 920.
4 S. L. Burkett and M. E. Davis, Chem. Mater., 7 (1995) 1453.
5 A. Corma, Chem. Rev., 97 (1997) 2373.
6 W. O. Haag, Stud. Surf. Sci. Catal., 84 (1994) 1375.
7 D. J. Parrillo, C. Pereira, G. T. Kokotailo and R. J. Gorte, Catalysis, 138 (1992) 337.
8 M. E. Davis, Microporous Mesoporous Mater., 21 (1998) 173.
9 S. L. Burkett and M. E. Davis, J. Phys. Chem., 98 (1994) 9647.
10 D. A. Young, US Pat. 3, 329, 480, 1967.
11 S. M. Kuznicki, US Pat. 4, 853, 202, 1989.
12 S. M. Kuznicki and A. K. Thrush, Eur. Pat. 0405978A1, 1990.
13 M. W. Anderson, O. Terasaki, T. Ohsuna, A. Philippou, S. P. MacKay, A. Ferreira, J. Rocha and S. Lidin, Nature, 367 (1994) 347.
14 M. W. Anderson, O. Terasaki, T. Ohsuna, P. J. O. Malley, A. Philippou, S. P. MacKay, A. Ferreira, J. Rocha and S. Lidin, Philos. Mag., B 71 (1995) 813.
15 A. Nastro, D. T. Hayhurst and S. M. Kuznicki, Stud. Surf. Sci. Catal., 98 (1995) 22.
16 T. Kr. Das, A. J. Chandwadkar and S. Sivasanker, Chem. Commun., (1996) 1105.
17 C. C. Pavel, D. Vuono, L. Cantazaro, P. De Luca, N. Bilba, A. Nastro and J. B. Nagy, Micropor. Mesopor. Mat., 56 (2002) 227.
18 J. Rocha, A. Ferreira, Z. Lin and M. W. Anderson, Micropor. Mesopor. Mat., 23 (1998) 253.
19 H. Xu, Y. Zhang and A. Navrotsky, Micropor. Mesopor. Mat., 47 (2001) 285.
20 L. Lv, F. Su and X. S. Zhao, Micropor. Mesopor. Mat., 76 (2004) 113.
21 X. Yang, J. P. Paillard, H. F. W. J. van Breukelen, H. Kessler and E. Duprey, Micropor. Mesopor. Mat., 46 (2001) 1.
22 X. Liu and J. K. Thomas, Chem. Commun., (1996) 1435.
23 C. C. Pavel, I. Asaftei, G. Iofcea, P. De Luca, D. Vuono, J. B. Nagy, A. Nastro and N. Bilba, E. van Steen, L. H. Callanan and M. Claeys, Eds., Full Proceedings of 14th International Zeolite Conference, Cape Town, South Africa, 25–30 April, 2004, p. 334 (Book of Abstracts); ISBN: 0-958-46636-x (CD-ROM), 1-920-01724-0.
24 P. De Luca and A. Nastro, H. Chon, S.-K. Ihen, Y. S. Uls, Eds., Progress in Zeolite and Microporous Materials, Studies in Surface Science Catalysis, Vol. 105, Elsevier, Amsterdam 1997, p. 221.
25 V. P. Valtchev and S. Mintova, Zeolites, 14 (1994) 697.
26 V. P. Valtchev, Chem. Commun., (1994) 730.
27 V. P. Valtchev, J. Chem. Soc., Chem. Commun., (1994) 261.
28 T. Kr. Das, A. J. Chandwadkar, A. P. Budhkar and S. Sivasanker, Microporous Mater., 5 (1996) 401.
29 M. W. Anderson, A. Philippou, Z. Lin, A. Ferreira and J. Rocha, Angew. Chem. Int. Ed. Engl., 34 (1995) 1003.
30 W. J. Kim, S. D. Kim, H. S. Jung and D. T. Hayhurst, Micropor. Mesopor. Mat., 56 (2002) 89.
31 C. C. Pavel, J. B. Nagy, N. Bilba, A. Nastro, C. Perri, D. Vuono, P. De Luca and I. V. Asaftei, Micropor. Mesopor. Mat., 71 (2004) 77-85.
32 C. C. Pavel, P. De Luca, N. Bilba, J. B. Nagy and A. Nastro, Thermochim. Acta, 435 (2005) 213.
33 D. Vuono, C. C. Pavel, P. De Luca, J. B. Nagy and A. Nastro, J. Therm. Anal. Cal., 80 (2005) 589.
34 Gy. Onyestyák, F. Lónyi and J. Valyon, J. Therm. Anal. Cal., 79 (2005) 561.

DOI: 10.1007/s10973-006-8040-1